(29) Berry, G. C.; Orofino, T. A. *J. Chem. Phys.* **1964**, *40*, 1614.
(30) Hadjichristidis, N.; Fetters, L. J., unpublished results.
(31) Prud'homme, J.; Roovers, J. E. L.; Bywater, S. *Eur. Polym. J.* **1972**, *8*, 901.
(32) This figure has appeared previously as Figure 12 in Burchard, W.; Kajiwara, K.; Nerger, D.; Stockmayer, W. H. *Macromolecules* **1984**, *17*, 222. The polyisoprene segment molecular weight for 18/46/152 given in that reference is incorrect; see Table I of this paper for the correct value.
(33) Mazur, J.; McCrackin, F. *Macromolecules* **1977**, *10*, 326.
(34) Khokhlov, A. R. *Polymer* **1978**, *19*, 1387.
(35) Khokhlov, A. R. *Polymer* **1981**, *22*, 447.
(36) Daoud, M.; Cotton, J. P. *J. Phys. (Les. Ulis, Fr.)* **1982**, *43*, 531.
(37) Miyake, A.; Freed, K. F. *Macromolecules* **1983**, *16*, 1228.
(38) Birshtein, T. M.; Zhulina, E. B. *Polymer* **1984**, *25*, 1453.
(39) Vlahos, C. H.; Kosmas, M. K. *Polymer* **1984**, *25*, 1607.

Neutron Scattering Studies of the Chain Conformation of Poly(methyl methacrylate) Deformed below the Glass Transition Temperature

M. Dettenmaier,*†§ A. Maconnachie,‡ J. S. Higgins,‡ H. H. Kausch,§ and T. Q. Nguyen§

Laboratoire de Polymères, Ecole Polytechnique Fédérale de Lausanne, CH-1007 Lausanne, Switzerland, and Department of Chemical Engineering, Imperial College of Science and Technology, London SW7 1BY, U.K. *Received November 28, 1984*

ABSTRACT: The technique of neutron scattering from mixtures of protonated and deuterated molecules has been used to analyze the conformation of chains in poly(methyl methacrylate) (PMMA) plastically deformed in uniaxial tensile tests. Measurements were conducted on samples that had been stretched to extension ratios of α = 2.0–2.3 in a temperature range of T = 60–120 °C. The magnitude of the scattering vector covered a range of $0 < q < 6$ nm^{-1}. The results obtained in the low-q range demonstrate that on the scale of the radius of gyration the deformation is approximately affine in the macroscopic strain tensor for long chains (M_w = 170 000 and 250 000) but markedly nonaffine for very short ones (M_w = 6000). In the intermediate- and high-q range the scattering curve of unstretched PMMA is compared with the scattering curve of stretched PMMA measured perpendicular to the draw axis. The results suggest that pronounced nonaffine modes of plastic deformation are active in regions of less than 2.5 nm.

1. Introduction

Considerable theoretical and technological interest has been focused in the past on the deformation and fracture of glassy polymers. However, the underlying molecular deformation mechanisms are still not very well understood. Most of the information available has been derived from measurements of macroscopic parameters such as stress, strain, and birefringence. The results obtained are generally discussed on the basis of deformation models that start from specific assumptions on the relation between macroscopic and molecular strains (see, e.g., ref 1 and 2). In the affine deformation model it is assumed that these strains are identical on any molecular level, i.e., that the transformation of the distance vector between any pair of molecular segments is affine in the macroscopic strain tensor. In the case of glassy polymers having a nonuniform strain distribution the affine deformation model has been applied to well-defined deformation zones such as shear bands[3] and craze fibrils.[4] The limits of applicability of the affine deformation model are not known at present. In fact, even if this model is valid on sufficiently large molecular scales, it must break down on very small ones because of the existence of intra- and intermolecular hindrances for the conformational rearrangement.

The relation between macroscopic and molecular strains may be established experimentally by using neutron scattering (NS) for the analysis of the conformational rearrangement of chain molecules. Most of the experiments have been conducted on amorphous polymers stretched above the glass transition temperature T_g. Very little is known on the chain conformation of amorphous polymers deformed below T_g. Recently, Lefebvre et al.[5] studied by small-angle neutron scattering (SANS) the chain conformation in shear bands of polystyrene deformed plastically under compression. They reported the existence of nonaffine modes of plastic deformation. According to Lefebvre et al.,[5] the deformation process does not affect the radius of gyration of the molecules within shear bands produced at low strain rates and at higher temperatures. This result has been attributed to the activation of a diffusional mode of plasticity. The isolation of shear bands from the surrounding matrix material and their study by NS cause severe experimental problems. Therefore, measurements on material deformed plastically under different conditions may be useful in examining the affine deformation model. For this reason NS experiments have been conducted on poly(methyl methacrylate) (PMMA), which may be highly deformed plastically in uniaxial tensile tests. The measurements reported in this paper cover a large q range ($0 < q < 6$ nm^{-1}) where information is obtained on both the radius of gyration of the molecules and the local arrangement of chain segments.

2. Experimental Section

Sample Preparation. To study the chain conformation of polymers NS measurements are generally conducted on mixtures of unlabeled (protonated) and labeled (deuterated) molecules. The two types of PMMA were prepared by radical polymerization of conventional and deuteriomethyl methacrylate, with benzoyl peroxide and dodecylmercaptan as initiator and transfer agent, respectively. The microtacticity of molecules of PMMA polymerized under these conditions has been analyzed by high-resolution

† Present address: Max-Planck-Institut für Polymerforschung, D-6500 Mainz, West Germany.
§ Laboratoire de Polymères, Ecole Polytechnique Fédérale de Lausanne.
‡ Department of Chemical Engineering, Imperial College of Science and Technology.

0024-9297/86/2219-0773$01.50/0 © 1986 American Chemical Society

Table I
Characteristics of Samples Used for NS

sample	x^D	M_w^D	U^D	M_w^H	U^H	T_g, °C
A	0.0465	158000	0.28	2400000	1.50	111
B	0.0400					125
	0.2000					123
	0.3750	232000	1.05	229000	0.98	124
	0.5000					123
	0.9600					121
C	0.9570	232000	1.05	5600	0.35	121

NMR. They contain about 78% racemic and 22% meso diads with average sequence lengths of 4.5 and 1.3 diads, respectively. To avoid imperfections from molding, a first series of samples (A) was prepared by using the technique of Kirste et al.:[6] After fractionation by dissolution in tetrahydrofuran and precipitation in methanol, the deuterated polymer was dissolved in the protonated monomer, which was then polymerized with the initiator and transfer agent indicated above. The thermal treatment of the samples during and after polymerization was identical with that described by Kirste et al.[6] The characteristics of sample A are summarized in Table I. x^D is the fraction of deuterated monomer units. M_w^D and M_w^H are the molecular weights of the deuterated and protonated chains, respectively. Their polydispersities are characterized by U^D and U^H, respectively, where $U = M_w/M_n - 1$. M_w and U were measured by GPC. The values of x^D, M_w^D, and M_w^H were chosen to ensure (1) the polymerization technique described above, (2) low coherent background scattering from voids, (3) large plastic deformation, and (4) evaluation of the radius of gyration from measurements at short sample–detector distances. Sample A was difficult to analyze at large q, where the coherent scattering from the small amount of deuterated molecules becomes very weak as compared to the incoherent scattering of the protonated matrix. Therefore, high-concentration mixtures of protonated and deuterated molecules (samples B) were prepared by using a different technique. Since molding turned out not to be a crucial point for (3), protonated and deuterated PMMA was dissolved in dioxane and after freeze-drying of the solution the samples were compression molded for 6 min at 180 °C. The samples are characterized in Table I. Their values of M_w^D, M_w^H, U^D, and U^H result from a compromise between (3) and (4). Evidently, the number of monomers per protonated and deuterated chain must be approximately equal when high-concentration mixtures are investigated. An identical technique was employed to prepare sample C, whose characteristics are included in Table I. For all the samples the glass transition temperature, measured by DSC at a heating rate of 10 K/min, is listed in Table I. Because of a small amount of residual monomer (≈1%) due to the preparation technique, sample A has a lower glass transition temperature as compared to samples B and C.

Tensile Experiments. For tensile tests, dumbbell-shaped specimens with a central portion of 25 mm in length, 4 mm in width, and 1.0–1.5 mm in thickness were milled from the cylinders and sheets obtained after polymerization and molding, respectively. The specimens were polished by conventional metallographic techniques with Al_2O_3 polishing solutions. Each sample was marked with a series of ink spots. The elongation of the sample was then determined between the ink spots before and after drawing. The tensile tests were conducted with a nominal strain rate of 6×10^{-4} s^{-1}.

Neutron Scattering Experiments. The experiments were carried out at the Institut Laue-Langevin in Grenoble, France, using the small-angle scattering instruments D11, D16, and D17. The details of the instruments and the data analysis have been given elsewhere.[7,8] The detector distances and wavelengths ranged from 10.66 m and 1.00 nm to 1.00 m and 0.45 nm. The largest wavelength distribution amounted to $\Delta\lambda/\langle\lambda\rangle \approx 10\%$. For the NS experiments the central portion of each stretched sample was cut into pieces 15 mm in length which were fixed in a sample holder such as to cover the diaphragm completely. Before being analyzed the data were corrected for detector response using water and for sample absorption. The scattering from water was also used to normalize the intensities. For convenience sectors of 20° were chosen on the two-dimensional detector to evaluate the scattering intensities of anisotropic samples parallel and perpendicular to the draw axis.

Background Scattering. The differential scattering cross section per unit volume of a mixture of deuterated and protonated molecules having the same number of monomer units is given by[9,10]

$$I(\mathbf{q}) = (a_D - a_H)^2 N_0 n x^D (1 - x^D) P(\mathbf{q}) + \frac{N_0}{4\pi}[x^D \sigma_{inc}^D + (1 - x^D)\sigma_{inc}^H] + \frac{N_0}{4\pi}[x^D(\sigma_{coh}^D)^{1/2} + (1 - x^D)(\sigma_{coh}^H)^{1/2}]^2 \langle\rho\rho\rangle$$

a_D and a_H denote the scattering lengths per deuterated and protonated monomer, respectively. N_0 is the total number of monomers per unit volume and n is the number of monomer units per chain. The single-chain form factor, P, is a function of the scattering vector $\mathbf{q}$ with

$$q = |\mathbf{q}| = (4\pi/\lambda) \sin(\theta/2)$$

where λ and θ respectively denote the wavelength of the neutrons and the scattering angle. σ_{inc}^D, σ_{inc}^H, σ_{coh}^D, and σ_{coh}^H are the incoherent and coherent scattering cross sections of the deuterated and protonated monomer units. $\langle\rho\rho\rangle$ denotes the density fluctuations in Fourier space.

$I(\mathbf{q})$ consists of three terms: (1) the coherent scattering from single chains, (2) the incoherent scattering from deuterated and protonated chains, and (3) the coherent scattering from density fluctuations. The scattering from the deuterated and protonated matrix has been used to determine the incoherent (2) and coherent (3) background scattering according to the equation given above.[10] The scattering from density fluctuations is angular independent and does not significantly contribute to the total amount of background scattering up to $q \simeq 3$ nm^{-1}. In this q range $I(\mathbf{q})$ is approximately given by

$$I(\mathbf{q}) = (a_D - a_H)^2 N_0 n x^D (1 - x^D) P(\mathbf{q}) + x^D I^D + (1 - x^D) I^H$$

where I^D and I^H denote the total scattering intensities of the deuterated and protonated matrix, respectively. At $q \geq 3$ nm^{-1} the coherent scattering from density fluctuations becomes increasingly important, resulting in a maximum of I^D at $q \simeq 9$ nm^{-1}.

3. Scattering Theory

After subtraction of the incoherent scattering and the coherent scattering from density fluctuations, the differential scattering cross section per unit volume of a mixture of deuterated and protonated molecules having the same number of monomer units is given by

$$I(\mathbf{q}) = (a_D - a_H)^2 N_0 n x^D (1 - x^D) P(\mathbf{q}) \quad (1)$$

$P(\mathbf{q})$ is obtained by Fourier transformation of the distribution functions $W(\mathbf{r}_{ij})$ for the vectors $\mathbf{r}_{ij}$ connecting the molecular units i and j:

$$P(\mathbf{q}) = \frac{1}{n^2} \sum_{i,j=1}^{n} \int e^{i\cdot\mathbf{q}\mathbf{r}_{ij}} W(\mathbf{r}_{ij})\, d\mathbf{r}_{ij} \quad (2)$$

Equation 2 may be used to establish a simple relation between the scattering behavior of chains before and after affine deformation. By definition the deformation is affine when all vectors $\mathbf{r}_{ij}$ are transformed into vectors $\mathbf{r}_{ij}^* = \alpha\mathbf{r}_{ij}$, where α is the macroscopic deformation tensor. Provided the deformation is uniaxial and occurs at constant volume ($|\alpha| = 1$), α may be written in the form

$$\alpha = \begin{pmatrix} \alpha^{-1/2} & 0 & 0 \\ 0 & \alpha^{-1/2} & 0 \\ 0 & 0 & \alpha \end{pmatrix}$$

where α is the extension ratio along the draw axis. Since

$$W^*(\mathbf{r}_{ij}) = W(\alpha^{-1}\mathbf{r}_{ij}) \quad (3)$$

where W and W^* are the distribution functions before and after deformation, eq 2 yields for the corresponding form factors the relation

$$P^*(\mathbf{q}) = P(\alpha\mathbf{q}) \quad (4a)$$

or

$$P^*(\mathbf{q}) = P(\mathbf{q}^*) \quad (4b)$$

with $\mathbf{q}^* = \alpha\mathbf{q}$. For uniaxially deformed samples it is convenient to measure under conditions where $\mathbf{q}$ is parallel and perpendicular to the draw axis. Equations 3 and 4 yield for the corresponding form factors

$$P_\parallel^*(q) = P(\alpha q) \quad (5a)$$

$$P_\perp^*(q) = P(\alpha^{-1/2}q) \quad (5b)$$

In the previous part of this section the distribution function $W(\mathbf{r}_{ij})$ has not been specified. In fact, it is not possible to give an analytical expression for $W(\mathbf{r}_{ij})$ that is valid over the whole range of $\mathbf{r}_{ij}$. However, for large $\mathbf{r}_{ij}$ the distribution function inevitably becomes Gaussian provided that the chain possesses some flexibility. Several authors[11-13] have treated the scattering behavior of affinely deformed Gaussian coils. Inserting the Gaussian distribution function into eq 2 and allowing for a Schultz distribution of the molecular weight, eq 4 yields

$$P^*(\mathbf{q}) = \frac{2}{(U+1)v^2}[(Uv+1)^{-1/U} + v - 1] \quad (6)$$

where $v = (U+1)^{-1}\langle R_{e_q}^2\rangle_z q^2$. The average is taken over all conformations and molecular weights. $\langle R_{e_q}^2\rangle_z$ is defined by the equation

$$\langle R_{e_q}^2\rangle_z = \frac{3}{2n^2}\sum_{i,j=1}^{n}\langle(\mathbf{e}_q\mathbf{r}_{ij})^2\rangle_z \quad (7)$$

and can be designated as three times the mean square of the inertial distance of the molecular units with respect to a plane defined by the unit vector $\mathbf{e}_q = \mathbf{q}/q$ and passing through the center of gravity of the molecule. Provided the sample is isotropic, for example if $\alpha = 1$, $\langle R_{e_q}^2\rangle$ is independent of $\mathbf{e}_q$ and coincides with the mean square of the radius of gyration

$$\langle R_{iso}^2\rangle_z = \frac{1}{2n^2}\sum_{i,j=1}^{n}\langle r_{ij}^2\rangle_z$$

Since eq 6 has been derived under the assumption of an affine deformation, eq 7 may be written in the form

$$\langle R_{e_q}^2\rangle_z = |\alpha\mathbf{e}_q|^2\langle R_{iso}^2\rangle_z \quad (8)$$

For a Schultz distribution of the molecular weight the z average is converted into the weight average by means of the relation

$$\langle R^2\rangle_w = \frac{U+1}{2U+1}\langle R^2\rangle_z \quad (9)$$

$\langle R_{e_q}^2\rangle_z$ may be evaluated from the scattering at low q without any specific assumption on $W(\mathbf{r}_{ij})$. In the low-q range ($v < 1$) eq 2 and 4 lead to the well-known formula

$$P^{*-1}(\mathbf{q}) = 1 + \langle R_{e_q}^2\rangle_z q^2/3 \quad (10)$$

For uniaxially deformed samples, $\mathbf{e}_q$ is conveniently chosen parallel and perpendicular to the draw axis, which yields $\langle R_\parallel^2\rangle$ and $\langle R_\perp^2\rangle$, respectively. Together with $\langle R_{iso}^2\rangle$ these quantities may be used to define a molecular extension ratio

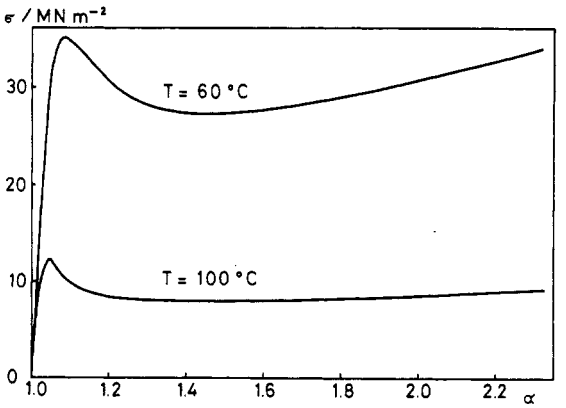

Figure 1. Nominal stress, σ, vs. extension ratio, α, for sample A drawn at 60 and 100 °C.

$$\alpha_{mol} = \frac{\langle R_\parallel^2\rangle^{0.5}}{\langle R_{iso}^2\rangle^{0.5}} = \frac{\langle R_{iso}^2\rangle}{\langle R_\perp^2\rangle} \quad (11)$$

which is identical with the macroscopic extension ratio, α, provided the deformation is affine. This follows directly from eq 8. In the intermediate- and high-q range Kratky plots are generally used to represent the scattering data. In the asymptotic limit of high q the plot $F^* = n_w P^*(\mathbf{q})q^2$ vs. q reaches a plateau given by (eq 6)

$$F^* = \frac{2}{|\alpha\mathbf{e}_q|^2\langle R_{iso}^2\rangle_w/n_w} \quad (12)$$

4. Results and Discussion

4.1. Deformation Behavior. The deformation and orientation of glassy PMMA have been extensively investigated in the literature.[14-18] From these studies it is well-known that PMMA like most other glassy polymers may deform in either a brittle or ductile manner depending on molecular weight, temperature, strain rate, and the applied stress field. To ensure high extension ratios samples were stretched at temperatures $T \geq 60$ °C. Nominal stress–strain curves are shown in Figure 1 for two drawing temperatures. In this temperature range PMMA deforms by the formation of diffuse shear zones which broaden and finally merge, resulting in optically homogeneous material as the extension ratio attains $\alpha \approx 2.0$. NS experiments were conducted on samples stretched to $\alpha = 2.0$–2.3. Extension ratios of about this magnitude are observed in necks and in unstressed craze fibrils of PMMA.[15,19] The range of accessible α is limited by two factors. At lower values the strain distribution is nonuniform because of the existence of shear zones. As a consequence, the interpretation of the scattering data in terms of existing deformation models requires a detailed knowledge of the strain distribution function, which is generally unknown. In particular, SANS measurements in the low-q range involve other moments of this function than measured macroscopically. At higher α intrinsic void formation[20] may cause severe experimental problems, and finally rupture intervenes.

4.2. Scattering at Low q. Information on the radius of gyration of the molecules has been derived from SANS measurements at low q. These measurements were conducted on mixtures of protonated and deuterated chains with largely different (samples A and C) and approximately equal (sample B) number of monomer units (see also Table I). In the first type of sample one species of molecules always forms a diluted component. Under this

Table II
Results Obtained at Low q

sample	M_w	$\langle R_{iso}^2\rangle_w^{0.5}$, nm	T, °C	$\langle R_\parallel^2\rangle_w^{0.5}$, nm	$\langle R_\perp^2\rangle_w^{0.5}$, nm	α_{mol} $\langle R_\parallel^2\rangle_w^{0.5}/\langle R_{iso}^2\rangle_w^{0.5}$	α_{mol} $\langle R_{iso}^2\rangle_w/\langle R_\perp^2\rangle_w$	α
A	171 000 ± 14 000	10.5 ± 0.5	60	20.4 ± 1.8	7.5 ± 0.4	1.9 ± 0.2	2.0 ± 0.2	2.1 ± 0.1
	170 000 ± 15 000		100	20.4 ± 2.0	7.6 ± 0.4	1.9 ± 0.2	1.9 ± 0.2	2.1 ± 0.1
B	244 000 ± 8000	13.5 ± 0.7	80		9.0 ± 0.2		2.3 ± 0.2	2.1 ± 0.1
	252 000 ± 8000		100		9.8 ± 0.2		1.9 ± 0.2	2.3 ± 0.1
	252 000 ± 7000		110		9.8 ± 0.2		1.9 ± 0.2	2.3 ± 0.1
	243 000 ± 8000		120		9.3 ± 0.2		2.1 ± 0.2	2.0 ± 0.1
C	6000 ± 500	2.0 ± 0.1	100	3.3 ± 0.2		1.7 ± 0.1		2.3 ± 0.1

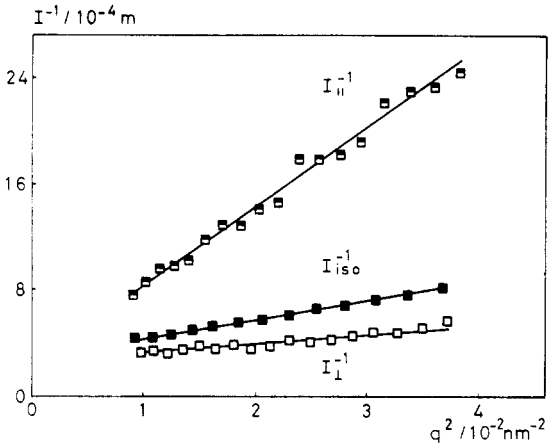

Figure 2. Plot of I^{-1} vs. q^2 of the scattering curves of sample A measured at low q. The reciprocal scattering intensities of the unstretched sample and of the stretched sample (T = 60 °C, α = 2.1) measured parallel and perpendicular to the draw axis are I_{iso}^{-1}, $I_\parallel^{-1}$, and $I_\perp^{-1}$, respectively.

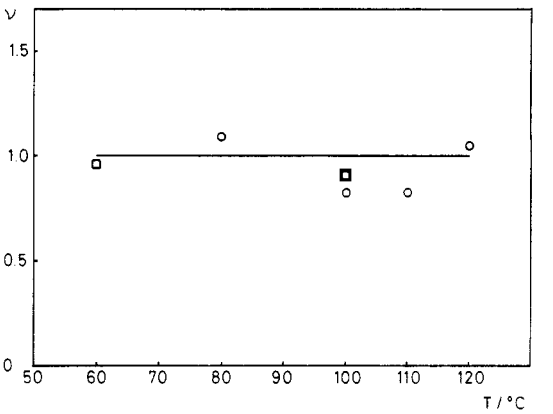

Figure 3. Ratio of the molecular and macroscopic extension ratio, $\nu = \alpha_{mol}/\alpha$, vs. drawing temperature, T, for samples A ((□) T_g = 111 °C) and B ((○) T_g = 123 °C).

condition eq 1 may be applied where $P(\mathbf{q})$ is approximately equal to the single-chain form factor of the diluted component. The correction for mismatched molecules according to Summerfield et al.[21,22] taking into account the single-chain form factor of the matrix component does not significantly affect the subsequent results. The second type of sample enables measurements over the whole concentration range, x^D, with maximum scattering intensities at x^D = 0.5. Measurements conducted on samples with various x^D demonstrated the validity of eq 1. Therefore, in the subsequent part of this paper experimental results obtained for x^D = 0.5 will be presented and discussed as being representative for the whole ensemble B in Table I.

Figure 2 shows plots of the form I^{-1} vs. q^2 for unstretched and stretched PMMA measured parallel and perpendicular to the draw axis. In the low-q range these plots yield straight lines that may be analyzed in terms of $\langle R_{iso}^2\rangle_z$, $\langle R_\parallel^2\rangle_z$, $\langle R_\perp^2\rangle_z$, and M_w on the basis of the scattering theory outlined in section 3. To a first approximation eq 10 may be used for this analysis. However, since $I_\parallel$ involves υ much larger than 1, more accurate results are obtained from a fit of eq 6 to the scattering data. The z-average square of the radius of gyration and the weight-average molecular weight remain in eq 1 and 6 as fitting parameters when U is taken from GPC measurements (Table I). The z average has been converted into the weight average by using eq 9. The results are listed in Table II.

The molecular weight given in Table II is the average value obtained from I_{iso}, $I_\parallel$, and $I_\perp$. For all samples the molecular weights measured by SANS (Table II) and GPC (Table I) agree within less than 10%. The systematic deviation that occurs must be assumed to reflect the imprecision in the calibration of either of the instruments.

The radii of gyration of the unstretched molecules and the molecular weights listed in Table II yield $\langle R_{iso}^2\rangle_w/n_w$ = 0.070 nm², which compares well with the value of 0.074 nm² obtained by Kirste et al.[6] O'Reilly et al.[23] have recently reported a value of 0.063 nm².

Together with $\langle R_{iso}^2\rangle_w^{0.5}$ the values of $\langle R_\parallel^2\rangle_w^{0.5}$ and $\langle R_\perp^2\rangle_w^{0.5}$ measured parallel and perpendicular to the draw axis, respectively, may be used to calculate the molecular extension ratio, α_{mol} (eq 11). In Table II the values of α_{mol} are compared with the macroscopic extension ratio, α, of samples stretched at various temperatures, T. The experimental errors in α_{mol} and α are about 10% and 5%, respectively. The results obtained for sample A demonstrate that the value of α_{mol} derived from measurements parallel to the draw axis agrees very well with that derived in the perpendicular direction. For samples B and C the evaluation of the scattering data in the parallel and perpendicular direction, respectively, caused severe problems: in the first case because of the large molecular dimensions and in the second case because of intense scattering from voids. Therefore, the experimental results listed in Table II for the stretched samples B and C are confined to only one particular direction.

The molecular extension ratios, α_{mol}, of samples A and B are situated close to the macroscopic extension ratio, α, over the whole range of drawing temperatures. This is demonstrated further in Figure 3, where the ratio $\nu = \alpha_{mol}/\alpha$ is plotted as a function of the drawing temperature, T. The experimental points yield $\langle\nu\rangle$ = 0.94, which is only slightly below the value of ν = 1 corresponding to an affine deformation. In view of the results of Lefebvre et al.[5] it is particularly important to note that ν is not affected by increasing the drawing temperature to temperatures of only a few degrees below T_g.

It is interesting to compare the deformation behavior of amorphous polymers below and above T_g. Several authors[23-26] have investigated by SANS the chain confor-

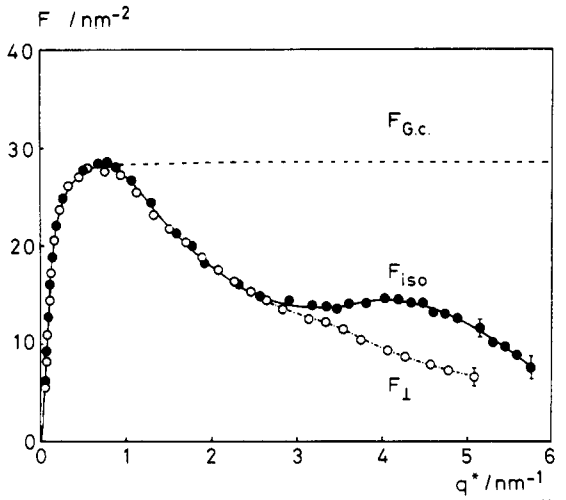

Figure 4. Kratky plot of $F = n_w P(q^*)q^{*2}$ vs. $q^* = \alpha_{mol}^{-1/2}q$ for unstretched sample B ((●) F_{iso}) and stretched sample B measured perpendicular to the draw axis ((○)$F_\perp$). The scattering function of Gaussian coils (F_{Gc}) is included for comparison.

mation in un-cross-linked amorphous polymers deformed above T_g. The results of these experiments agree with the affine deformation model provided molecules are stretched under conditions where the conformational relaxation is slow as compared to the time scale of the deformation experiment.[25,26] This is the case for long chains stretched at temperatures close to T_g. In view of these results the deformation behavior of glassy PMMA observed in these studied seems to be reasonable.

The deformation behavior of short chains, even when embedded into a high molecular weight matrix, is markedly nonaffine. This is demonstrated in Table II for sample C. The molecular extension ratio of the low molecular weight component is much smaller than α, indicative of the existence of nonaffine deformation mechanisms on small molecular scales. This result will be discussed further in the subsequent section in conjunction with the discussion of the scattering behavior of PMMA in the intermediate- and high-q range.

4.3. Scattering at High q. Information on the local arrangement of chain segments is obtained from the scattering behavior at intermediate and high q. In this q range only high-concentration mixtures of protonated and deuterated PMMA could be analyzed with sufficiently high accuracy. Therefore, the subsequent discussions are confined to specimens of series B among which that with $x^D = 0.5$ will serve as an example (see also section 4.2). In the intermediate- and high-q range, NS experiments were conducted on samples stretched at 100 °C. Figure 4 shows results that have been obtained for the unstretched sample (F_{iso}) and for the stretched one in the direction perpendicular to the draw axis ($F_\perp$). The scattering function $F(q^*) = n_w P(q^*)q^{*2}$ has been plotted as a function of $q^* = \alpha_{mol}^{-1/2}q$ (eq 5b). The theoretical scattering function $F_{Gc}(q^*)$ for undeformed and affinely deformed Gaussian coils is included in Figure 4 for comparison. $F_{Gc}(q^*)$ has been calculated by inserting into eq 6 the radius of gyration measured in the low-q range.

The subsequent discussion will first focus on the scattering behavior of unstretched PMMA as compared with previous results reported by Kirste et al.[6] and by Yoon and Flory.[28] The scattering function F_{iso} exhibits two maxima, one in the intermediate-q range and one in the high-q range. The scattering function for Gaussian coils, F_{Gc}, closely fits the experimental data up to the first maximum, in accordance with SANS results obtained by Kirste et al.[6] and with Monte Carlo calculations performed by Yoon and Flory[28] on the basis of the rotational isomeric state theory. At the first maximum, F_{iso} attains the plateau value of F_{Gc} (eq 12). The strong departure from the scattering behavior of Gaussian coils at higher q, also observed by Kirste et al.[6] and recently by O'Reilly et al.,[23] has been analyzed in great detail by Yoon and Flory.[28-31] According to Yoon and Flory, this behavior must be rationalized in terms of the specific conformation statistics of the large amount of racemic diads present in "atactic" PMMA. The strong preference of racemic diads for the trans,trans conformation together with the inequality of the skeletal bond angles at C^α and CH_2 cause a maximum in the characteristic ratio that is reflected in the first maximum of $F_{iso}(q)$. The second maximum of $F_{iso}(q)$ has not been considered in detail by Yoon and Flory. It may be assumed to be related to the spiralization of the persistence vector in syndiotactic PMMA.[30] Qualitatively, the shape of the scattering function $F_{iso}(q)$ measured by NS is very similar to that calculated by Yoon and Flory.[28] However, the observed maxima occur at larger values of q than those exhibited by the calculated curve.

In the plot F vs. q^* the scattering functions F_{iso} and $F_\perp$ superimpose surprisingly well over a large q^* range including the region of the first maximum. In particular, in the q^* range below this maximum $F_\perp$ like F_{iso} is well approximated by the scattering function of Gaussian coils (eq 6). When $F_\perp$ and F_{iso} are considered as functions of q, they scale as α_{mol}:1 at the first maximum (see also eq 12). At $q^* > 2.5$ nm^{-1} the scattering functions $F_\perp$ and F_{iso} deviate increasingly. Since the second maximum in F_{iso} results from correlations along the chain axis, it is not surprising that this maximum reduces to a tiny hump in $F_\perp$. The fact that this hump is situated at smaller q^* indicates that α_{mol} in $q^* = \alpha_{mol}^{-1/2}q$ overestimates the real deformation of chains on small molecular scales. The results presented in Figure 4 seem to indicate the existence of pronounced nonaffine modes of plastic deformation at $q^* \geq 2.5$ nm^{-1}, corresponding to Bragg distances of $d \leq 2.5$ nm in the unstretched sample. The nonaffine deformation of very short chains with $\langle R_{iso}\rangle_w^{0.5} = 2$ nm (Table II) is consistent with these findings. In fact, short chains must be assumed to have a higher susceptibility to nonaffine modes of deformation than chain sequences of equivalent length forming part of much longer chains.

The deformation behavior observed on small molecular scales has to be expected since severe geometrical constraints are imposed by bond lengths, bond angles, and hindrance potentials. The existence of these constraints is also reflected in the orientation behavior of chain segments, which is generally described by nonaffine deformation models such as the "pseudoaffine" deformation model of Ward.[1,18]

5. Concluding Remarks

Valuable information on the deformation of chains in highly extended glassy PMMA has been derived from NS experiments covering a large q range. Measurements at low q demonstrate that the deformation of long chains is approximately affine on the scale of the radius of gyration. In contrast, the deformation of very short chains is markedly nonaffine. Measurements in the intermediate- and high-q range indicate the existence of pronounced nonaffine modes of plastic deformation in regions of less than 2.5 nm. Future experiments on the temperature and strain rate dependence of this value may yield a deeper insight into the molecular deformation mechanism. In particular, the interesting question arises how this value is affected by the glass transition. Unfortunately, the NS data that are available at present for amorphous polymers

stretched above T_g do not allow the question to be answered.

Acknowledgment. The financial support of the Swiss National Science Foundation is gratefully acknowledged. We thank Prof. P. J. Flory for fruitful discussions and are indebted to Dr. B. J. Schmitt (BASF AG) and Dr. W. Wunderlich (Röhm GmbH.) for providing the deuteriomethyl methacrylate. The GPC measurements of low molecular weight PMMA were kindly performed by Dr. M. Stickler (Röhm GmbH.). We are also indebted to Dr. R. E. Ghosh and Dr. A. Wright (ILL, Grenoble) for their help with the experiments and data evaluation.

Registry No. PMMA (homopolymer), 9011-14-7; neutron, 12586-31-1.

References and Notes

(1) Ward, I. M. "Mechanical Properties of Solid Polymers"; Wiley-Interscience: New York, 1983.
(2) Kausch, H. H. "Polymer Fracture", 1st ed.; Springer-Verlag: Berlin, 1978 (2nd ed. to be published).
(3) Donald, A. M.; Kramer, E. J. *Polymer* **1982**, *23*, 1183.
(4) Donald, A. M.; Kramer, E. J. *J. Polym. Sci., Polym. Phys. Ed.* **1982**, *20*, 899.
(5) Lefebvre, J. M.; Escaig, B.; Picot, C. *Polymer* **1982**, *23*, 1751.
(6) Kirste, R. G.; Kruse, W. A.; Ibel, K. *Polymer* **1975**, *16*, 120.
(7) (a) Timmins, P. A.; May, R. P. ILL Internal Report 81 TI 535. (b) Maier, B., Ed. "Neutron Research Facilities at the ILL High Flux Reactor"; Institut Laue-Langevin: Grenoble, France, Dec 1983.
(8) Ghosh, R. E. ILL Internal Report 81 GH 29T.
(9) Tangari, C.; Summerfield, G. C.; King, J. S.; Berliner, R.; Mildner, D. F. R. *Macromolecules* **1980**, *13*, 1546.
(10) Gawrisch, W.; Brereton, M. G.; Fischer, E. W. *Polym. Bull.* **1981**, *4*, 687.
(11) Benoit, H.; Duplessix, R.; Ober, R.; Daoud, M.; Cotton, J. P.; Farnoux, B.; Jannink, G. *Macromolecules* **1975**, *8*, 451.
(12) Pearson, D. S. *Macromolecules* **1977**, *10*, 696.
(13) Ullman, R. *J. Chem. Phys.* **1979**, *71*, 436.
(14) Rehage, G.; Goldbach, G. *Angew. Makromol. Chem.* **1967**, *9*, 125.
(15) Allison, S. W.; Andrews, R. D. *J. Appl. Phys.* **1967**, *38*, 4164.
(16) Beardmore, P. *Philos. Mag.* **1969**, *19*, 389.
(17) Matsushige, K.; Radcliffe, S. V.; Baer, E. *J. Appl. Polym. Sci.* **1976**, *20*, 1853.
(18) Kahar, N.; Duckett, R. A.; Ward, I. M. *Polymer* **1978**, *19*, 136.
(19) Kambour, R. P. *Polymer* **1964**, *5*, 143.
(20) Dettenmaier, M. *Adv. Polym. Sci.* **1983**, *52/53*, 57.
(21) Summerfield, G. C. *J. Polym. Sci., Polym. Phys. Ed.* **1981**, *19*, 1011.
(22) Tangari, C.; King, J. S.; Summerfield, G. C. *Macromolecules* **1982**, *15*, 132.
(23) O'Reilly, J. M.; Teegarden, D. M.; Wignall, G. D. *Macromolecules* **1985**, *18*, 2747.
(24) Picot, C.; Duplessix, R.; Decker, D.; Benoit, H.; Boué, F.; Cotton, J. P.; Daoud, M.; Farnoux, B.; Jannink, G.; Nierlich, M.; de Vries, A. J.; Pincus, P. *Macromolecules* **1977**, *10*, 436.
(25) Maconnachie, A.; Allen, G.; Richards, R. W. *Polymer* **1981**, *22*, 1157.
(26) Boué, F.; Nierlich, M.; Jannink, G.; Ball, R. *J. Phys. (Paris)* **1982**, *43*, 137.
(27) Hadziioannou, G.; Wang, L.-H.; Stein, R. S.; Porter, R. S. *Macromolecules* **1982**, *15*, 880.
(28) Yoon, D. Y.; Flory, P. J. *Macromolecules* **1976**, *9*, 299.
(29) Yoon, D. Y.; Suter, U. W.; Sundararajan, P. R.; Flory, P. J. *Macromolecules* **1975**, *8*, 784.
(30) Yoon, D. Y.; Flory, P. J. *Polymer* **1975**, *16*, 645.
(31) Yoon, D. Y.; Flory, P. J. *J. Polym. Sci., Polym. Phys. Ed.* **1976**, *14*, 1425.

Brillouin Scattering and Side-Group Motions of Poly(alkyl methacrylates) above and below the Glass Transition

B. Y. Li,[†] D. Z. Jiang,[‡] G. Fytas,[§] and C. H. Wang*

Department of Chemistry, University of Utah, Salt Lake City, Utah 84112.
Received September 24, 1985

ABSTRACT: The effect of side-group motions on the Rayleigh–Brillouin spectra of poly(alkyl methacrylates) has been investigated. Various samples of poly(methyl methacrylate), poly(ethyl methacrylate), and poly(butyl methacrylate) with different molecular weights and different T_g are used to investigate (1) the relation between the Brillouin line width maximum and T_g, (2) the effect of main-chain and side-group motions on the Brillouin linewidth, and (3) the temperature dependence of the Landau–Placzek ratio. To further demonstrate the effect of side-group motion in poly(butyl methacrylate) (PBMA), Brillouin scattering of stretched PBMA films has also been investigated.

Introduction

The use of light scattering to study amorphous solids (glasses) dates back to the time of Lord Rayleigh[1] and has continued to the present day with every increasing activity. However, it is the development of modern optical techniques involving the use of a single-mode laser for excitation and a Fabry–Perot interferometer or a digital correlator for spectral analysis that makes it feasible to obtain information about the dynamic processes underlying formation of the glass state.

Dynamic light scattering from an isotropic medium (liquid or glass) arises from thermodynamic fluctuations in the local density, anisotropy, and, in the case of a multicomponent system, concentration. These fluctuations give rise to variations in the local dielectric constant tensor. In a light scattering experiment dealing with an amorphous system, the wavelength of the laser light employed for excitation is long compared with the intermolecular distance; it is thus useful to treat the scattering system as a continuous medium in which thermally excited collective excitations perturb the local dielectric constant tensor. For an isotropic medium such as the poly(alkyl methacrylate) system presently considered in this paper, the dominant contribution to the light scattering intensity arises from density fluctuations, as the contribution from anisotropy fluctuations to the scattered light is negligible. The scattering spectrum arising from density fluctuations is known as the Rayleigh–Brillouin spectrum.

The Rayleigh–Brillouin spectrum from a polymer melt consists of a central component and a pair of shifted sidebands. The intensity ratio between the central com-

[†] Institute of Applied Chemistry, Academia Sinica, Changchun, Jilin, China.
[‡] Department of Chemistry, Jilin University, Changchun, Jilin, China.
[§] Department of Chemistry, University of Crete, Iraklion, Crete, Greece.

0024-9297/86/2219-0778$01.50/0 © 1986 American Chemical Society